# A role for the spectrin superfamily member Syne-1 and kinesin II in cytokinesis

**Jun Fan and Kenneth A. Beck***

Department of Cell Biology and Human Anatomy, School of Medicine, University of California, Davis, CA 95616, USA
*Author for correspondence (e-mail: kabeck@ucdavis.edu)

## Summary

Expression of a dominant negative fragment of the spectrin family member Syne-1 causes an accumulation of binucleate cells, suggesting a role for this protein in cytokinesis. An association of this fragment with the C-terminal tail domain of the kinesin II subunit KIF3B was identified by yeast two-hybrid and co-precipitation assays, suggesting that the role of Syne-1 in cytokinesis involves an interaction with kinesin II. In support of this we found that (1) expression of KIF3B tail domain also gives rise to multinucleate cells, (2) both Syne-1 and KIF3B localize to the central spindle and midbody during cytokinesis in a detergent resistant and ATP sensitive manner and (3) Syne-1 localization is blocked by expression of KIF3B tail. Also, membrane vesicles containing syntaxin associate with the spindle midbody with identical properties. We conclude that Syne-1 and KIF3B function together in cytokinesis by facilitating the accumulation of membrane vesicles at the spindle midbody.

Key words: Kinesin, Cytokinesis, Mitosis, Golgi, Spectrin, Vesicle transport.

## Introduction

Synaptic nuclear envelope protein-1 (Syne-1) is an unusually large spectrin family member that is expressed in several alternatively spliced forms in a range of tissues (Apel et al., 2000; Gough et al., 2003; Mislow et al., 2002; Zhang et al., 2001). Initially identified as a binding protein for the acetylcholine receptor in skeletal muscle (Apel et al., 2000), isoforms of Syne-1 have been found to localize to the nuclear envelope and several investigators have found evidence that Syne-1 functions at the inner nuclear membrane (Mislow et al., 2002; Zhang et al., 2002; Zhang et al., 2001). An alternative function for Syne-1 is suggested by the observation that functional perturbations of a related protein in *Caenorhabditis elegans*, ANC-1, gives rise to nuclear positioning defects (Starr and Han, 2002), indicating that Syne-1 might function at the outer surface of the nuclear envelope and facilitate specialized nuclear movements and localization. More recently, we have found evidence for Golgi localization of Syne-1 (Gough et al., 2003). Two distinct Golgi binding sites on Syne-1 have been identified and overexpression of one of these sites causes alterations in the structure of the Golgi complex (Gough et al., 2003). In light of this latter observation, we have proposed that one of the functions of Syne-1 is to facilitate the close association of Golgi and nuclear envelope observed in skeletal muscle cells (Gough et al., 2003). Thus, Syne-1 appears to be a multifunctional protein with potential roles in inner nuclear envelope function, cytoplasmic nuclear positioning and the maintenance of Golgi structure.

Mitotic cell division requires the coordinated action of a large number of cellular proteins and cell biological processes. While many proteins involved in the regulation of mitotic events are specialized proteins that are synthesized only during mitosis, many others are present throughout the cell cycle and serve alternative roles during mitosis and interphase. For example, microtubules facilitate vesicle transport and organelle distribution during interphase (Kreis, 1990), whereas during mitosis microtubules, rearranged to form the mitotic spindle, serve alternate roles (Mitchison, 1988). During early stages of mitosis the spindle facilitates the segregation of chromosomes (Nasmyth, 2002) and organelles (Thyberg and Moskalewski, 1998), and it is well documented that the positioning of the mitotic spindle determines the orientation of the cleavage furrow (Rappaport, 1986). The structural integrity of the spindle is also essential for completion of the last stage of cell division: cytokinesis (Wheatley and Wang, 1996). In dividing animal cells, the antiparallel overlapping polar microtubules of the mitotic spindle form a discrete domain called spindle mid-zone or central spindle (Severson and Bowerman, 2002). Following metaphase, numerous proteins essential for cytokinesis, including kinesin-like motors, associate with this domain (Hirose et al., 2001; Adams et al., 1998; Cooke et al., 1987; Matuliene and Kuriyama, 2002). Later, at cytokinesis, this structure is compacted to form the midbody matrix. Mutations in proteins that localize to the central spindle and midbody result in an improper assembly of the midbody matrix and the failure of cytokinesis, giving rise to binucleate cells (Matuliene and Kuriyama, 2002).

There is also evidence that the cellular machinery that facilitates vesicular trafficking in interphase cells also plays an important role during mitosis (for a review, see O'Halloran, 2000). For instance, the completion of cytokinesis requires an increase of cell membrane surface area at the cleavage site (Danilchik et al., 1998). This addition of membrane during cytokinesis probably involves proteins that function in vesicular transport from Golgi to plasma membrane, such as

the t-snare syntaxin (Jantsch-Plunger and Glotzer, 1999) and the exocyst complex (Wang et al., 2002). Further, as with plant cell cytokinesis, the later stages of cytokinesis in animal cells might require microtubule-dependent transport of vesicles along spindle-microtubules to the cleavage site (Skop et al., 2001).

Here we provide evidence that Syne-1 acquires a specialized role during cell division. We show that Syne-1 localizes to the spindle mid-zone and is essential for the completion of cytokinesis. We also show that Syne-1 binds the kinesin II subunit KIF3B and that spindle association of Syne-1 occurs through this plus-end directed motor protein. Because the fundamental function attributed to all spectrin family members is that of linking membranes to the cytoskeleton, we propose that the role for Syne-1 in cytokinesis is to attach membrane vesicles to the mitotic spindle and the midbody through a kinesin-like motor, thereby facilitating vesicular transport to the cleavage zone. In support of this we show evidence that membrane vesicles containing the t-snare syntaxin 4 also associate with the central spindle and midbody through interactions with Syne-1-kinesin II.

## Materials and Methods

### Antibodies

Rabbit polyclonal antibodies (SN120, SN357 #1 and #2) were generated against distinct Syne-1 peptides as described previously (Gough et al., 2003). Anti-KIF3B polyclonal antibody MPSR-BSA was provided by Bruce Schnapp (Oregon Health Sciences University). Monoclonal $\alpha$-tubulin (Sigma-Aldrich, St Louis, MO), anti-E-cadherin (BD Transduction Laboratories, Palo Alto, CA) anti-syntaxin-4 (BD Transduction Laboratories), rabbit anti-protein disulfide isomerase polyclonal antibody (StressGen Biotechnologies, San Diego, CA), polyclonal rabbit anti-Giantin (Covance, Berkeley, CA), anti-Myc (Clontech, Palo Alto, CA) and anti-influenza hemeaglutinin (HA) antibodies (Clontech) were purchased and used according to the manufacturer's instructions.

### Cells culture and transfection

Cells (HeLa, NRK and COS) were cultured in Dulbecco's modified Eagle's medium (DMEM) supplemented with 10% fetal bovine serum, 100 U ml$^{-1}$ penicillin, and 100 µg ml$^{-1}$ streptomycin at 37°C in a humidified atmosphere with 5% CO$_2$. For the transient expression assay, $1.6 \times 10^6$ cells were transfected in 100 mm dishes using PolyFect or SuperFect transfection reagent (Qiagen, Santa Clarita, CA) according to the manufacturer's recommendation for 20-24 hours and then fixed and processed for immunofluorescence staining. The amount of plasmid-DNA was kept constant (4 µg per 100 mm dish, 3 µg per 60 mm dish).

To generate enriched mitotic cells, HeLa and NRK cells were synchronized at G2–M by treating them with thymidine (2 mM) in DMEM overnight. Following this, nocodazole (Sigma-Aldrich, St Louis, MO) was added to a final concentration of 500 ng ml$^{-1}$ in DMEM. Cells were grown for 5 hours, and then washed twice with complete medium. Afterwards, cells were allowed to grow for 45 to 60 minutes in complete medium, fixed and processed for immunofluorescence staining.

For immunoblot assay, HeLa cells were transfected for 24 hours in 100 mm dishes and extracted in TX-100 extraction buffer [150 mM NaCl, 1% Triton X-100, 50 mM Tris-HCl (pH 7.4)] and with protease inhibitors (0.5 mg ml$^{-1}$ EDTA-Na$_2$, 1 mg ml$^{-1}$ pefabloc SC, 10 µg ml$^{-1}$ leupeptin, 10 µg ml$^{-1}$ pepstatin, and 1 µg ml$^{-1}$ aprotinin). Protein concentrations were determined using the Pierce BCA protein assay (Pierce Chemical, Rockford, IL).

### Yeast two-hybrid assay

The Gal4-based Matchmaker® two-hybrid system III from Clontech (Clontech, Palo Alto, CA) was used for the yeast two-hybrid assays. Plasmid vectors pGBKT7 and pACT2 encoding the Gal4-binding domain (Gal4-BD) and Gal4-activing domain (Gal4-AD), respectively, were used to express hybrid proteins. A library screening by yeast mating was performed to seek proteins that interact with Syne-1. The bait was the fragment GSSF1 cloned into the Gal4-BD vector pGBKT7 and transformed into the yeast strain AH109 (MATα) (see below for details), whereas the screened library was constructed from human kidney cDNA inserted into Gal4-AD vector pACT7 and transformed into MATα yeast strain Y187. The mating mixture was spread on high-stringency plates (SD/–Ade/–His/–Leu/–Trp/X-α-Gal) virtually eliminating false positive interactions. Putative positive colonies from the first screening were streaked on SD/–Leu/–Trp/X-α-Gal plates three times. The final blue colonies were streaked on SD/–Ade/–His/–Leu/–Trp/X-α-Gal to verify that they maintained the correct phenotype (Ade+/His+/Mel1+). These Gal4-AD plasmids were recovered in bacteria strain HB101. DNA from positive clones was isolated and sequenced.

Syne-1 cDNA fragments corresponding to GSSF1 (nucleotides 13220-14437 of GenBank BK000543) and GSSF5 (n17240-17924) were amplified by PCR to give rise to cDNAs flanked by *Nde*I and *Bam*HI sites. These amplified fragments were digested with *Nde*I and *Bam*HI, purified and subcloned into pGBKT7 to construct fusion proteins with the DNA binding domain of the GAL4 protein. DNA sequencing was used to verify that these constructs were in the correct reading frame and that no nucleotide mutations had taken place. These DNA-binding-domain fusion constructs were introduced into strain AH109 (MATα) according to the instructions provided by the manufacturer (Clontech, Palo Alto, CA). To ensure that the constructs did not activate reporter genes (HIS3 and MEL1) the assay was performed with bait alone before the library screen. Expression of these fusion proteins was also confirmed by western blotting with an antibody against the myc epitope tag also encoded in the bait construct. Our data showed that the GSSF1 construct could be used as bait.

### Plasmid construction

cDNAs encoding GSSF1 and GSSF 5 were amplified from pGBKT7-GSSF1 and pGBKT7-GSSF5, respectively, by PCR and ligated into pCMV-HA vectors using *Sal*I and *Kpn*I restriction sites. The full-length human KIF3B was cloned from cDNA derived from the human kidney cell line HEK293 using primers 5′acgcgtcgaccatgtcaaagttgaaaagctcaga-3′ and 5′-acgcggtaccttactttggaaccagcccccgagact-3′. The KIF3B-motor region was amplified from the KIF3B clone by using primers 5′-acgcgtcgaccatgtcaaagttgaaaagctca-3′ (forwards) and 5′cggggtaccagcaatctcttcctggaattctcg-3′ (backwards). Both primers were modified by adding a *Sal*I site (forwards primer) and a *Kpn*I site (backwards primer) to their 5′end. Both amplified cDNAs were digested with *Sal*I and *Kpn*I, purified and then liga ted into the pCMV-myc vector. The KIF3B tail region was retrieved from pACT7-KIF3B tail by using *Sfi*I and *Xho*I sites, and then inserted into pCMV-myc vector via *Sfi*I and *Xho*I restriction sites. To ensure a correct reading frame, all constructs were sequenced.

To generate the GFP fusion proteins, sequences encoding GSSF1 and GSSF5 were amplified by PCR using primers 5′-atgaatgagactgctgagctgc-3′ and 5′-ttagaacctttgacactgactg-3′; 5′-atcaagatgaaggcatccg-3′ and 5′-ttatcatctggtcttcagcaggtg-3′, respectively. Amplified fragments were ligated into TOPO-N-GFP (Invitrogen, Carlsbad, CA). All clones were confirmed by DNA sequencing.

### Immunofluorescence microscopy

Cells were grown on poly-D-lysine-coated glass coverslips for immunofluorescence microscopy, fixed with 2% formaldehyde-PBS

(2.7 mM KCl, 1.5 mM KH$_2$PO$_4$, 137 mM NaCl, 8 mM Na$_2$HPO$_4$) for 10 minutes at room temperature, or with –20°C methanol for 3 minutes. Fixed cells were washed with PBS, permeablized in 0.5% Trition X-100 in PBS for 10 minutes at room temperature, and washed again with PBS. These lysed cells were then blocked in PBS with 0.2% (g ml$^{-1}$) bovine serum albumin (BSA) buffer containing 10% goat serum and 0.05 M aluminum chloride (blocking buffer) for 20 minutes. Blocked cells were then incubated with primary antibodies diluted in blocking buffer. After 1 hour at room temperature, cells were rinsed 3× with PBA with 0.2% (g ml$^{-1}$) BSA and incubated with fluoroscene isothiocyanate (FITC) or rhodamine-conjugated secondary antibodies, also diluted in blocking buffer. If required, cells were stained with 4′,6′-diamidino-2-phenylindole (DAPI) at 0.5 μg ml$^{-1}$. To prevent bleaching, coverslips were mounted on slides using Fluoromount-G. Specimens were examined under a Nikon E600 microscope equipped with epifluorescence optics using a 63× objective and an oil immersion lens (NA=1.3). For optical deconvolution microscopy, samples were examined using an Olympus IX70 inverted microscope fitted to an Applied Precision Delta Vision Restoration, DV3.0. Images were recorded using an Olympus 100× oil immersion lens (NA=1.4) and a Photometrics CH350 CCD camera (Roper Scientific, Acton, MA). Deconvolution and image analysis was performed using tools provided in the SoftWorx (version 2.5) software package (API, Issaquah, WA).

Image quantification (Figs 7 and 9) was performed with NIH image (version 1.63). Briefly, a rectangular area overlaying the midbody was defined and the mean pixel density was measured. The rectangular area was then dragged to a region immediately adjacent to the midbody to record the background cytoplasmic signal. Both of these measurements were normalized against specimen background by recording the mean pixel density in an equivalent area outside the perimeter of the cell. Plotted are the ratios of normalized midbody:cytoplsmic background signal, where a value of 1.0 corresponds to no detectable accumulation in the midbody (Figs 7 and 9).

### Fluorescence activated cell sorting

Cells were transfected with GFP-GSSF1 or GFP-GSSF5 or Superfect transfect reagent (Qiagen) alone according to the Superfect transfection manual. After a 24 hour transfection period, cells were trypsined, fixed in 0.5% paraformaldehyde in PBS for 20 minutes on ice and then washed in cold PBS. The cells were fixed, permeabilized in 90% methanol and 10% PBS (–20°C) and then stained with the DNA fluorochrome propidium iodide in PBS containing 0.1% Triton X-100 and 100 ng ml$^{-1}$ RNase A. Labeled cell populations were analyzed by fluorecence-activated cell sorting by detecting GFP and PI fluorescence using a MoFlo SN-1058 cell sorter (Cytomation, Ft. Collins, CO). The portion of GFP-positive cells containing twice the normal amount of DNA (2× DNA) were quantified.

### Western blots and immunoprecipitation

Total protein (~20 ug in sample loading buffer) was separated on a 7.5% SDS-PAGE gel using standard procedures and then electro-transferred to Immu-Blot PVDF membranes (BioRad, Hercules, CA) in 25 mM Tris (pH 8.3), 190 mM glycine, and 5% MeOH using a Bio-Rad transblot apparatus. Blots were blocked with PBS buffer containing 1% nonfat dry milk and 0.2% BSA for 1 hour at room temperature or overnight at 4°C, incubated in anti-KIF3B antibody (1:100 dilution) for 1 hour at room temperature and then washed in TTBS (100 mM Tris-HCl pH 7.4, 150 mM NaCl and 0.1% Tween-200). To visualize protein bands, blots were incubated in goat anti-rabbit IgG conjugated to horseradish peroxidase (HRP) for 1 hour, washed extensively and developed using ECL chemiluminescence reagents (Amersham, Piscataway, NJ).

Co-transfected COS-7 cells were washed with ice-cold PBS, scraped in buffer (150 mM NaCl, 1% Triton X-100, 50 mM Tris-HCl pH 7.4, 0.5 mg ml$^{-1}$ EDTA-Na$_2$, 1 mg ml$^{-1}$ pefabloc SC, 10 μg ml$^{-1}$ leupeptin, 10 μg ml$^{-1}$ pepstatin, and 1 μg ml$^{-1}$ aprotinin) with a rubber policeman, and collected in a 1.5 ml tube. Cells were lysed by passage through a 27-gauge needle 3-5 times and incubated on ice for 30 minutes. Lysates were spun down at 10,000 $g$ for 10 minutes at 4°C, and then the soluble material was used for subsequent immunoprecipitation. Approximately 250 μg of solubilized cell lysate was used for each immunoprecipitation. Briefly, 1 μg of antibody was added to 50 μl of 50% protein-A agarose beads and rotated for 3 hours at 4°C. The beads were washed three times with buffer, recovered by centrifuging at maximum speed in a benchtop microcentrifuge for 30 seconds, and then boiled for 5 minutes in 100 μl of Laemmli loading buffer. The resultant supernatant was subjected to SDS-PAGE and western blotting as described above.

## Results

### A role for Syne-1 and kinesin II in cytokinesis

To address the function of Syne-1 at the Golgi complex we have studied the expression of various recombinant fragments of the Syne-1 protein with the aim of identifying dominant negative inhibitors of Syne-1 function (Gough et al., 2003). One of the fragments identified by this approach, here referred to as GSSF1 (Fig. 1A), is located just upstream of the first Golgi binding site of Syne-1 and lacks homology to spectrin repeat domains, indicating that it represents a unique domain that is not found in other spectrin family members. While examining the effects of GSSF1 expression on Golgi structure and function, we noticed that cells expressing this fragment often contained two or more nuclei (Fig. 1B,C,E). Because this is a classic phenotype for a defect in cytokinesis we chose to examine this observation in more detail.

Fig. 1E (panels a-c) shows the nuclei of several examples of COS-7 cells transfected with GSSF1. All of the examples shown contain double nuclei. While nontransfected COS-7 cell cultures normally contain a limited number of bi- and multinucleate cells, the occurrence of multiple nuclei in cells transfected with GSSF1 was elevated noticeably. A count of DAPI stained COS-7 cells transfected with GSSF1 found that 20-30% of the cells were binucleate. To test whether the accumulation of multiple nuclei in cells transfected with GSSF1 might be because of preferential transfection of binucleate cells we expressed GSSF5, a fragment of Syne-1. We have found previously that expression of this fragment has no effect on Golgi structure and function (Gough et al., 2003). We did not find examples of multinucleate cells transfected with this fragment (Fig. 1E, panels d-f), illustrating the specificity of the effect observed with GSSF1.

To obtain a more quantitative assessment of the frequency of occurrence of multinucleate cells in GSSF1 tranfectants, we performed a fluorescence-activated cell sorting (FACS) experiment (Fig. 1D). HeLa cells, which have a lower baseline occurrence of multinucleate cells than COS-7, were transiently transfected with GFP-tagged GSSF1, then fixed and their nuclei were labeled with propidium iodide (see Materials and Methods). FACS analysis was then performed to isolate GFP-positive cell populations having twice the normal content of DNA, measured as propidium iodide fluorescence. For GSSF1 transfectants, the number of GFP-positive cells with the double amount of DNA (measured as a percentage of the total pool of transfectants) was almost two-fold higher than the equivalent
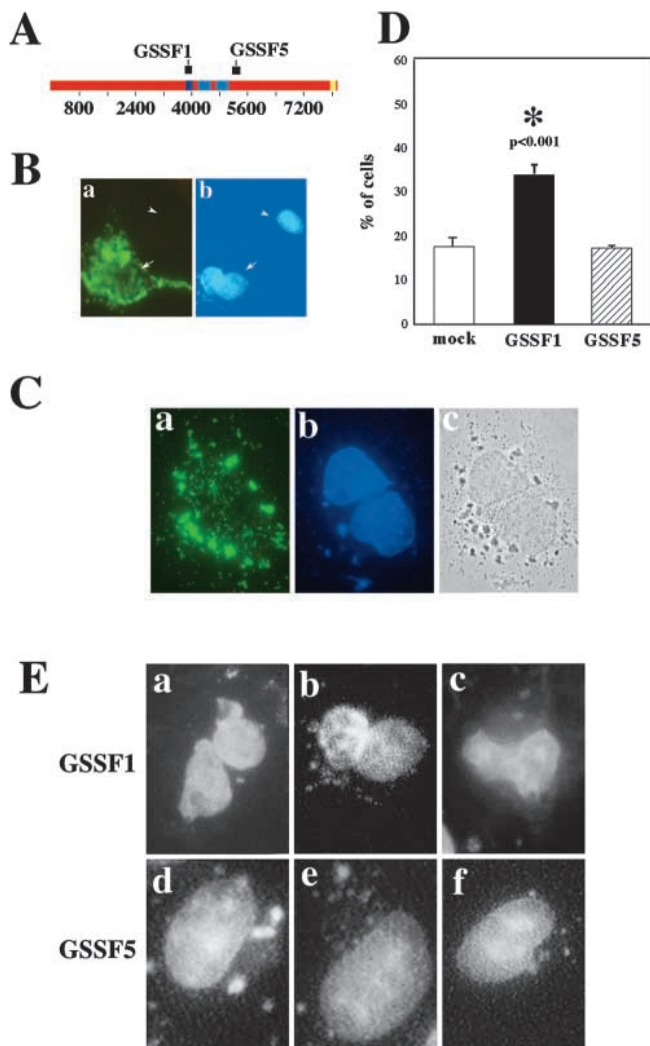
**Fig. 1.** Expression of the Syne-1 fragment GSSF1 blocks cytokinesis in animal cells. (A) A map of Syne-1 protein showing the positions of the two fragments used in these studies, the kinesin binding fragment GSSF1 and the control fragment GSSF5 that does not bind kinesin. Also shown are the two Golgi binding sites identified previously (light blue), the proposed nuclear envelope binding site (yellow) and the kinesin II binding site identified in this study (dark blue). (B) When COS-7 cells were transfected with GFP-tagged GSSF1 (a) and nuclei were stained with DAPI (b), we found that a large proportion of transfected cells (a and b, arrow) were binucleate, whereas untransfected cells remained mononucleate (a and b, arrowheads). (C) COS-7 cell transfected with GSSF1 (a), stained with DAPI (b), examined by phase contrast microscopy (c) appears as a single binucleate cell (rather than two adjacent mononucleate cells). (D) Fluorescence activated cell sorting (FACS) assay for binucleate cells. HeLa cells were transfected with GFP-GSSF1 (black bar), GSSF5 (striped bar) or mock transfected (white bar). GFP positive cells were isolated by fluorescence activated cell sorting and the proportion of total GFP-positive cell population possessing twice the normal amount of DNA was quantified by propidium iodide fluorescence. Because mock transfected cells do not express GFP, the proportion of the total cell population with twice the normal amount of DNA is given in percent. Error bars indicate standard deviation of triplicate FACS experiments (* indicates the statistically significant difference compared to the control obtained by Student's $t$-test). (E) DAPI-stained cells transfected with dominant-negative fragment GSSF1 (a-c), the control fragment GSSF5 (d-f).

population in mock transfected controls (Fig. 1D). HeLa cells transfected with GFP-tagged control fragment GSSF5, however, showed no increase in the number of cells with 2×-DNA content (Fig. 1D, GSSF5) compared to the mock-transfected control. Therefore, the increase in 2×-DNA content is specific for the GSSF1 fragment.

The basal level of 2×-DNA-positive cells observed in both mock- and GSSF5-transfected cultures (~17%) corresponds to the population of cells in G2 and M phases of the cell cycle. If mitosis is maintained at steady state in the transfected cell population, it can be assumed that G2 and M phase cells will be present in similar amounts in the controls and that only the excess (10-15%) would correspond to binucleate cells. By contrast, if entry into the cell cycle was restricted in transfected cells, and mitotic cells were consumed without replacement, the 10-15% difference would represent an underestimate of the number of binucleate cells deficient in cytokinesis. Several observations lead us to conclude that this latter case is occurring. First, if transfected cultures are allowed to grow for extended periods of time we observe a significant decease in the number of cells expressing the construct, suggesting that GSSF1 affects the general cell viability. This is to be expected. We have found that expression of this fragment in interphase cells alters Golgi structure and blocks retrograde vesicular transport from Golgi to endoplasmic reticulum (ER). Such effects would probably diminish the viability of interphase cells. Therefore, it would not be surprising if GSSF1 expression also diminished the capacity of cells to enter the cell cycle. We have found this to be true. FACS measurements of cells with >1× but <2× DNA content (cells in S phase) show a dramatic reduction in cells expressing GSSF1 (1.0±0.7% against 9.8±0.3%, GSSF5 control $P<0.001$). This indicates that S, G2 and M phase cells are indeed being consumed without replacement. The fact that we see an increase in the percentage of cells with 2× DNA content under these conditions therefore suggests that binucleate cells are making up a larger proportion of the cells with 2× DNA content. In support of this, a count of the bi- and mononucleate cells transfected with GSSF1 found that 25% of the cells were binucleate, indicating that a majority of the 2× DNA positive population measured by FACS corresponds to binucleate cells that are defective in cytokinesis. By contrast, it is very difficult to find examples of transfected cells in other stages of mitosis (i.e. metaphase and anaphase). We therefore conclude that our FACS analysis supports the general conclusion that GSSF1 expression gives rise to binucleate cells by blocking cytokinesis.

### Syne-1 fragment GSSF1 binds the kinesin II subunit KIF3B

The observation that GSSF1 expression gives rise to binucleate cells indicates that this region of Syne-1 is biologically active. We therefore performed a yeast two-hybrid screen of a human kidney cDNA library with this fragment to identify potential binding proteins of GSSF1 (see Materials and Methods). This screen resulted in the isolation of a partial cDNA encoding a C-teminal segment of the trimeric kinesin subunit KIF3B, a microtubule-based motor protein belonging to the kinesin II family. Members of this family are implicated in anterograde vesicular transport in
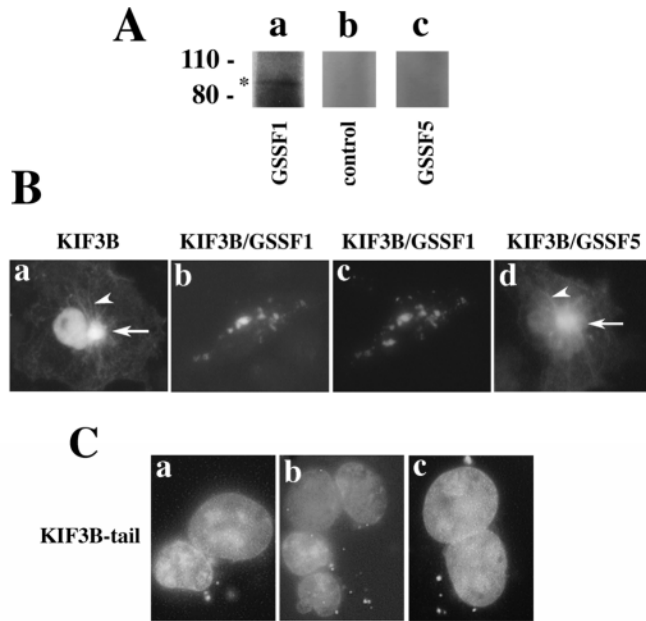
**Fig. 2.** (A) COS-7 cells were co-transfected with recombinant, full-length kinesin II tagged with a myc epitope and either recombinant HA-tagged GSSF1 (a,b) or GSSF5 (c). Immune complexes were precipitated with an anti-HA antibody (a,c) or a control IgG (b) and western blots were stained with anti-KIF3B. The recombinant kinesin II can be detected in immunoprecipitates from cells expressing GSSF1 (lane a, *) but not GSSF5 (lane c). GSSF5 was used here as a control because it does not bind KIF3B in the two-hybrid system (not shown). Electrophoretic mobilities of molecular weight markers of 110 and 80 kDa are indicated to the left of the figure. (B) Co-localization of GSSF1 and KIF3B. COS-7 cells were transfected with myc-KIF3B (a) or co-transfected with myc-KIF3B and HA-GSSF1 (b,c) or myc-KIF3B and HA-GSSF5 (d). Fixed cells were stained with antibodies to myc-KIF3B (a,b,d) or HA-GSSF1 (c). KIF3B localizes to the Golgi (a and d, arrows) and microtubules (a and d, arrowheads) in cells expressing KIF3B alone (a) and in cells transfected with both KIF3B and the control fragment GSSF5 (d). By contrast, when KIF3B is co-transfected with GSSF1, KIF3B distribution is altered and both proteins co-localize in punctate cytoplasmic structures. (C) DAPI-stained COS-7 cells transfected with C-terminal tail domain of KIF3B. Several examples of bi- and multinucleate cells are shown (a-c).

neurons (Yamazaki et al., 1995), an observation that is consistent with an association with Syne-1 functioning at the Golgi. To determine whether KIF3B can form a complex with GSSF1 in mammalian cells, we transfected COS-7 cells with epitope-tagged GSSF1, immunoprecipitated GSSF1 complexes with an epitope-tag-specific monoclonal antibody and performed protein blots of the precipitated complexes with antibodies against KIF3B (Fig. 2A). Using this approach we determined that immunoprecipitates of GSSF1 contained a polypeptide of the appropriate size (95 kDa) that reacted with anti-KIF3B antibody (Fig. 2A, lane a). By contrast, when this same experiment was performed with a control IgG, we did not observe a band in the immunoprecipitate that corresponded to KIF3B (Fig. 2A, lane b). Also, we have found that GSSF5 does not interact with KIF3B when assayed either by yeast two-hybrid screening (not shown) or by immunoprecipitation of extracts from cells expressing GSSF5

(Fig. 2A, lane c), illustrating the specificity of the observed GSSF1 interaction.

As an alternative approach to demonstrating an interaction of GSSF1 with KIF3B in intact cells, we introduced full-length recombinant KIF3B into COS-7 cells either alone or by co-transfection with GSSF1 and examined the distribution of the ectopic KIF3B (Fig. 2B). When full-length KIF3B is expressed alone it localizes to the Golgi complex (Fig. 2B, panel a, arrow) and to filamentous processes that resemble microtubules (Fig. 2B, panel a, arrow head), which is consistent with a potential function for KIF3B in microtubule-based vesicular transport from the Golgi. By contrast, upon co-transfection with GSSF1, ectopic KIF3B no longer localizes to these structures. Instead it is associated with punctate cytoplasmic structures containing GSSF1 (Fig. 2B, panels b, c). KIF3B distribution is not affected when co-transfected with the control fragment GSSF5 (Fig. 2B, panel d), again demonstrating the specificity of the GSSF1-KIF3B interaction. These results not only illustrate the ability of GSSF1 to interact with KIF3B, they also indicate that GSSF1 might act as a dominant negative inhibitor of KIF3B function.

To address the potential role for KIF3B in cytokinesis we expressed a truncated form of KIF3B that contained the C-terminal tail domain but lacked the N-terminal motor domain. This truncation is often used as a dominant negative inhibitor of kinesin function. Transfected cells were then screened by immunofluorescence microscopy to detect multinucleate cells (Fig. 2C). As observed with GSSF1, the expression of the KIF3B tail domain gave rise to an increased frequency of bi- and multinucleate cells, suggesting that both Syne-1 and KIF3B function in cytokinesis.

## Localization of Syne-1 during mitosis and cytokinesis

The accumulation of binucleate cells upon expression of GSSF1 and KIF3B tail domain clearly indicates a role for these proteins in mitotic cell division. Because the nuclei of affected cells, although duplicated, appear intact, we suspect that these proteins act by affecting cytokinesis and not earlier stages of mitosis. To gain additional information on the role that these two proteins might play in cytokinesis, we examined their distribution during the cell cycle by indirect immunofluorescence microscopy.

Using a Syne-1-specific anti-peptide antibody (SN120) that was previously shown to stain the Golgi complex in interphase cells (Gough et al., 2003), we found that during early phases of mitosis Syne-1 localizes to diffusely distributed punctate structures (Fig. 3a-d) reminiscent of the morphology and distribution of mitotic Golgi fragments (Shima et al., 1998). Throughout pro-metaphase (Fig. 3a,b) and metaphase (Fig. 3c,d) these punctate structures accumulate near the poles of the mitotic spindle (Fig. 3a,c, arrows), consistent with what is observed with Golgi markers at this stage. However, following metaphase, Syne-1 distribution diverges from the fate of typical Golgi markers and instead accumulates as a band of material localized to the center of the cell, bisecting the spindle (Fig. 3e,f). This distribution persists throughout the remaining mitotic stages (Fig. 3g-j) and is particularly evident during cytokinesis where the majority of Syne-1 accumulates at the midbody (Fig. 3i,j). Localization to the midbody is especially relevant to cytokinesis because this structure resides within the

region where opposing membranes of the cleavage furrow ingress and ultimately fuse to form separate daughter cells.

Close inspection of a high-magnification image of a mitotic NRK cell double-stained with SN120 and tubulin-specific antibodies revealed localization of Syne-1 to the mitotic spindle (Fig. 4a). Remarkably, Syne-1 was largely restricted to only the central part of the spindle (Fig. 4a, arrows). Using optical sectioning microscopy we examined the distribution of Syne-1 within a narrow focal plane, parallel to the long axis of the anaphase spindle (Fig. 4b). With this technique we found that Syne-1 localizes to microtubules of the central spindle in rows of discrete puncta. While the majority of Syne-1 resides at the spindle mid-zone, we also detected Syne-1 on additional punctate structures that associated with microtubules at more peripheral regions of the spindle, perhaps corresponding to Syne-1 complexes in transit through the central spindle. During cytokinesis some diffuse Syne-1 staining is found along the
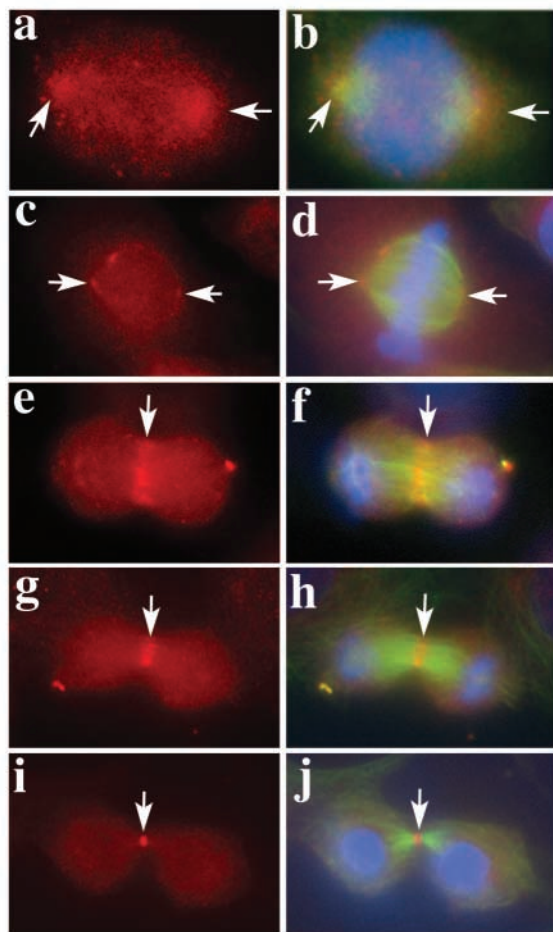
length of the condensed spindle (Fig. 4c-e), but the majority of spindle-associated Syne-1 is found as a compacted ring-like structure that encircles the midbody (Fig. 4d,e).

The mitotic spindle is comprised of two distinct classes of microtubules: polar microtubules that maintain the structure of the spindle and kinetochore microtubules that facilitate
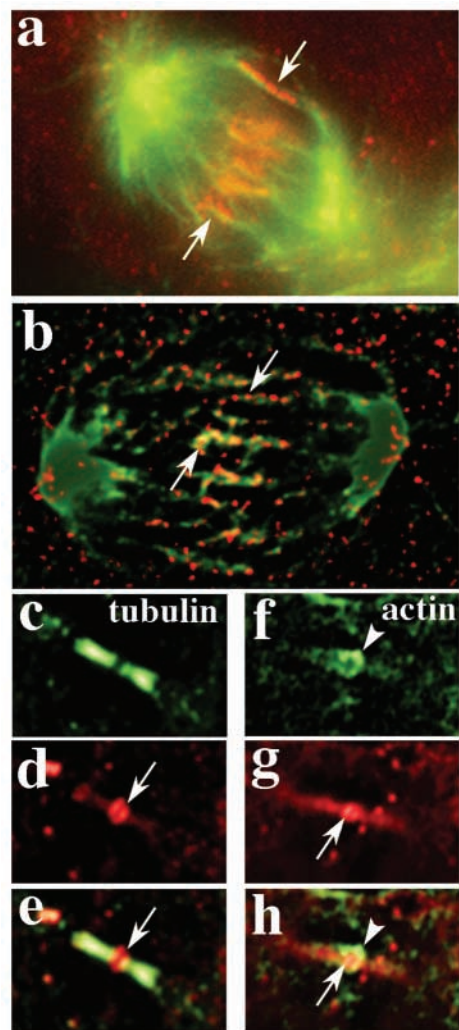


**Fig. 3.** Localization of Syne-1 during mitotic cell division. Mitotic cells were fixed and stained with anti-tubulin (green), polyclonal anti-Syne-1 (red) and DAPI (blue). Localization of Syne-1 during various stages of mitosis (a,c,e,g,i). Triple-staining of the same cells indicate the localization of Syne-1 relative to the mitotic spindle and chromosomes (b,d,f,h,j). At stages before and during metaphase (a-d) Syne-1 is localized at punctate structures typical for Golgi markers (a-d, arrows). After metaphase Syne-1 is localized at a band of material that bisects the central spindle (e-j). This localization persists through cytokinesis where midbody localization is observed (i and j).

**Fig. 4.** Syne-1 localizes to central spindle and midbody, but not to the contractile ring. Mitotic NRK cells, double-stained with anti-Syne-1 (red) (a,b,d,e,g,h) and either with anti-tubulin (green) (a-c,e) or with fluorescein phalloidin (green) (f,h). (a) Conventional fluorescence microscopy reveals that Syne-1 co-localizes with spindle-microtubules (arrows) and that its distribution during anaphase is restricted along the spindle to the central region. (b) High-resolution image generated by optical sectioning microscopy of an anaphase mitotic spindle, double stained with antibodies to tubulin (green) and Syne-1 (red), demonstrates that Syne-1 associates with the central spindle microtubules in the form of discrete puncta (c-e, arrows). An optical sectioning image of NRK cells entering cytokinesis double stained with antibodies to tubulin (c) and Syne-1 (d) (e is an overlay of c and d) illustrates that Syne-1 localizes to a ring-like structure that surrounds the spindle midbody (d and e, arrows).
(f-h) Fluorescein phalloidin stained actin of the contractile ring (f, arrowhead), which encircled the Syne-1 positive structure at the midbody (g, arrow). An Overlay (h) of f and g revealed that Syne-1 (h, arrow) did not localize to the contractile ring (h, arrowhead).

chromosome motility. We conclude that Syne-1 localizes to polar microtubules because central-spindle localization persist throughout anaphase as well as later stages (Fig. 4a,b and Fig. 3) when the kinetochore microtubules have regressed away from the central spindle. The mid-zone of the spindle corresponds to the region where polar microtubules overlap, and where opposing forces of the overlapping serve to hold the spindle together (Severson and Bowerman, 2002). Disruption of this region of the spindle after completion of metaphase leads to cytokinesis defects (Wheatley and Wang, 1996). Therefore, the localization of Syne-1 to this region of the mitotic spindle, known to be essential for cytokinesis, supports the conclusion that Syne-1 functions in cytokinesis.

While the localization of Syne-1 to the central spindle and midbody suggests that its potential role in cytokinesis is the consequence of spindle interactions, it is also possible that Syne-1, an actin binding protein (Zhang et al., 2002), functions in cleavage furrow ingression at the level of the actin-myosin contractile ring. To assess this potential function of Syne-1 we compared its localization during a late stage of mitosis with that of actin localized to the contractile ring by optical sectioning microscopy (Fig. 4f-h). As mentioned above, Syne-1 localizes to a compact ring-like structure that encircles the midbody during cytokinesis (Fig. 4d,g). Phalliodin stained actin also localizes to a ring surrounding the midbody (Fig. 4f, arrowhead), but this contractile ring is notably larger than the Syne-1 positive structure (compare Fig. 4f,g). A overlay of the two images (Fig. 4h) revealed that Syne-1 and actin localize to two distinct ring structures and that these ring structures are concentric, with the actin-containing contractile ring distal to the midbody and the Syne-1 positive ring nested between the spindle midbody and the contractile ring. Syne-1 is absent form the contractile ring. The close apposition of the contractile ring and midbody-localized Syne-1 suggests that Syne-1 serves to bind the encroaching contractile ring and tether it to the spindle, thereby facilitating the final stages of cytokinesis.
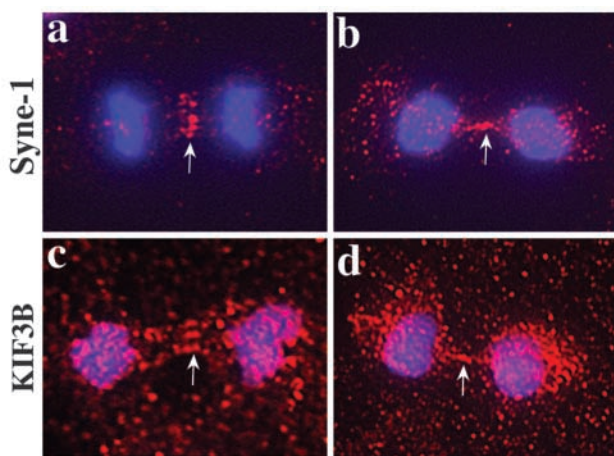


**Fig. 5.** Association of Syne-1 and kinesin II with central spindle and midbody is detergent resistant. NRK cells were extracted with Triton X-100 before fixation and then stained with anti-Syne-1 antibody (red) (a,b), for KIF3B with anti-kinesin II antibody (red) (c,d) and DAPI (blue). Both Syne-1 and kinesin II localized to detergent insoluble structures associated with the central spindle in anaphase (arrow) (a,c) and the midbody during cytokinesis (arrow) (b,d).

Antibodies against Syne-1 prominently stained structures associated with the spindle mid-zone and midbody, even in cells that had been extracted with 0.5% TX-100 before fixation (Fig. 5a,b), consistent with a tight association with the microtubule cytoskeleton. We reasoned that this association of Syne-1 with spindle-microtubules probably occurs through the association of Syne-1 with KIF3B discussed above. Indeed, previous studies that examined the distribution of the kinesin II homolog ($KRP_{(85/95)}$) in mitotic sea urchin embryos showed that it localizes to the central spindle during anaphase (Hensin et al., 1995), analogous to our observation of Syne-1 association (Figs 3, 4). To determine whether KIF3B localizes to these structures in mammalian cells, we stained detergent-extracted COS-7 cells with an antibody against KIF3B (Fig. 5c,d). KIF3B localized to the central spindle during anaphase (Fig. 5c) as well as the midbody during cytokinesis (Fig. 5d). As we have found with Syne-1, the association of KIF3B with these domains of the mitotic spindle occurred in the presence of detergent. The observation that Syne-1 and KIF3B co-localize at the central spindle and midbody in a detergent-resistant manner provided additional evidence that these two proteins might have similar or coordinated functions during the cell cycle.

To gain additional evidence for the proposal that the association of Syne-1 with the mitotic spindle occurs through interactions with KIF3B, we took advantage of the established ATP-dependence of kinesin-microtubule interactions (Fig. 6). In the presence of MgATP, kinesin dissociated from the spindle midbody (Fig. 6c). Likewise, the localization of Syne-1 to midbody was also greatly diminished when MgATP was available for hydrolysis by kinesin II (Fig. 6i). By contrast, the non-hydrolyzable ATP analog AMP-PNP, which should stabilize kinesin-microtubule interactions, had little effect on the localization of either KIF3B (Fig. 6e) or Syne-1 (Fig. 6k). In fact, the relative amount of both proteins residing at the midbody appeared to increase slightly in the presence of AMP-PNP, consistent with the known stabilizing effects of this agent on kinesin-microtubule interactions. These results support the conclusion that Syne-1 interacts with the mitotic spindle through kinesin II interactions.

As a more direct test of this idea, we examined the distribution of Syne-1 in mitotic NRK cells expressing the dominant negative tail domain of KIF3B (Fig. 7). Because our yeast two-hybrid screen indicated that Syne-1 interacts with kinesin II through the tail domain of the KIF3B subunit, we expected that overexpression of this domain would prevent the association of Syne-1 with the spindle midbody. As a control, we expressed full-length recombinant KIF3B. This full-length construct, unlike the tail domain, was expected to associate with spindle-microtubules and be incorporated into functional kinesin II trimers. As expected, expression of KIF3B tail domain resulted in significantly diminished accumulation of Syne-1 at the midbody during cytokinesis (Fig. 7d) compared to the full-length KIF3B control (Fig. 7b). To quantify these results we performed quantitative image analysis on multiple examples of KIF3B-expressing mitotic cells (Fig. 7e, see also Materials and Methods). In mock transfected cells, the average amount of Syne-1 that accumulated at the spindle mid-zone was twice as high as the amount of Syne-1 that was detected in the region directly adjacent to the midbody (data not shown). Upon expression of the full-length KIF3B, we observed even
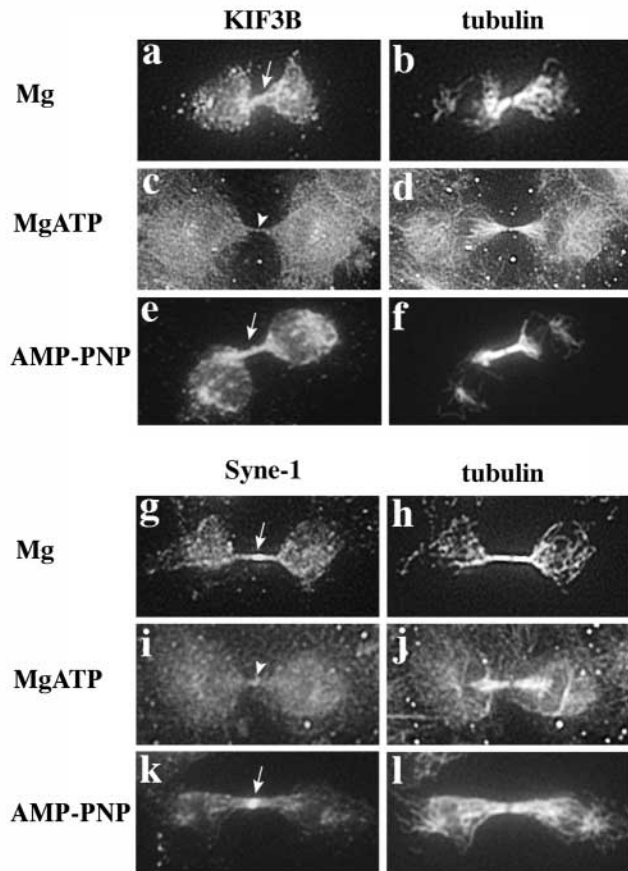
**Fig. 6.** Association of kinesin II and Syne-1 with the midbody is sensitive to ATP. To determine whether Syne-1 and kinesin II interactions with the mitotic spindle were coupled, distribution of Syne-1 (g,i,k) and kinesin II (a,c,e) was investigated in cells that had been detergent extracted in the presence of 10 mM MgSO$_4$ (a,b,g,h), 10 mM MgATP (c,d,i,j) or 10mM of a non-hydrolyzable ATP anolog AMP-PNP (e,f,k,l). Cells were stained with antibodies against KIF3B (a,c,e) or Syne-1 (g,i,k) and then double-stained with anti-tubulin antibody (b,d,f,h,j,l) to visualize the mitotic spindle. Localization of both kinesin II and Syne-1 are greatly reduced in the presence of ATP (indicated by arrowheads) (c,i) and slightly enhanced in the presence of AMP-PNP (indicated by arrows) (e,k).
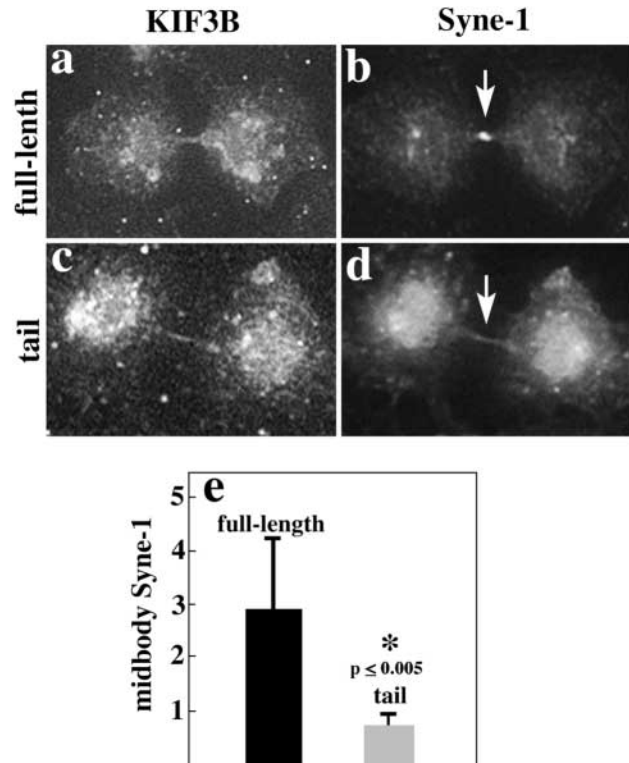


**Fig. 7.** KIF3B tail domain blocks Syne-1 localization to the midbody. (a-d) NRK cells transfected with myc-tagged KIF3B tail domain (c,d) or with full-length myc-KIF3B as a control (a,b). Cells were fixed and stained with anti-myc (a,c) to identify transfected cells, and with polyclonal SN120 to localize Syne-1 (b,d). While Syne-1 was concentrated at the midbody in cells transfected with the control full-length KIF3B (arrow) (b), it was significantly depleted from the midbody in cells transfected with KIF3B tail (arrow) (d). (e) To quantify this result, NRK cells transfected with KIF3B tail (tail) or with transfected with full-length KIF3B (full-length) were subjected to digital image analysis (see Materials and Methods). The amount of Syne-1 staining at the midbody (mean pixel density) was measured and is plotted as the ratio of midbody localized Syne-1 staining to background Syne-1 staining. Staining was measured in the cytoplasm directly adjacent to the midbody (error bars=standard deviation; * indicates the statistically significant difference from mock transfected cells by Student's *t*-test).

higher levels Syne-1 at the midbody (Fig. 7e, full-length), although statistical analysis revealed this apparent increase in midbody Syne-1 was not statistically significant (*P*=0.1). By contrast, upon expression of KIF3B tail domain, we observed a significant reduction in the level of Syne-1 localized to the midbody. Expression of this dominant-negative fragment of KIF3B served to reduce the amount of midbody Syne-1 to a level equivalent to that found in the surrounding cytoplasm (Fig. 7e, tail), indicating that Syne-1 was no longer localized preferentially to the midbody in these cells. These results confirm our proposal that KIF3B serves to link Syne-1 to the mitotic spindle.

## Interactions of membrane vesicles with Syne-1-kinesin during mitosis

A fundamental function of all spectrin family members is to link membranes to the cytoskeleton. With this in mind we reasoned that one potential function for Syne-1 and KIF3B in cytokinesis is to facilitate the association of membrane vesicles with the mitotic spindle. To test this idea we sought to identify membrane proteins that co-localize with Syne-1 and KIF3B on the central spindle and midbody. We chose three membrane marker proteins for these studies: Syntaxin, a t-snare involved in the targeting of membrane vesicles to the plasma membrane; E-cadherin, a cell adhesion molecule; and the ER-resident protein disulfide isomerase (PDI). Antibodies against these proteins were used to stain mitotic NRK cells to determine whether membrane vesicles containing these proteins associate with the mitotic spindle through Syne-1-KIF3B (Fig. 8). While both E-cadherin (Fig. 8c) and the ER marker PDI (Fig. 8b) showed no evidence of localizing to the spindle mid-zone, antibodies against syntaxin prominently stained this structure
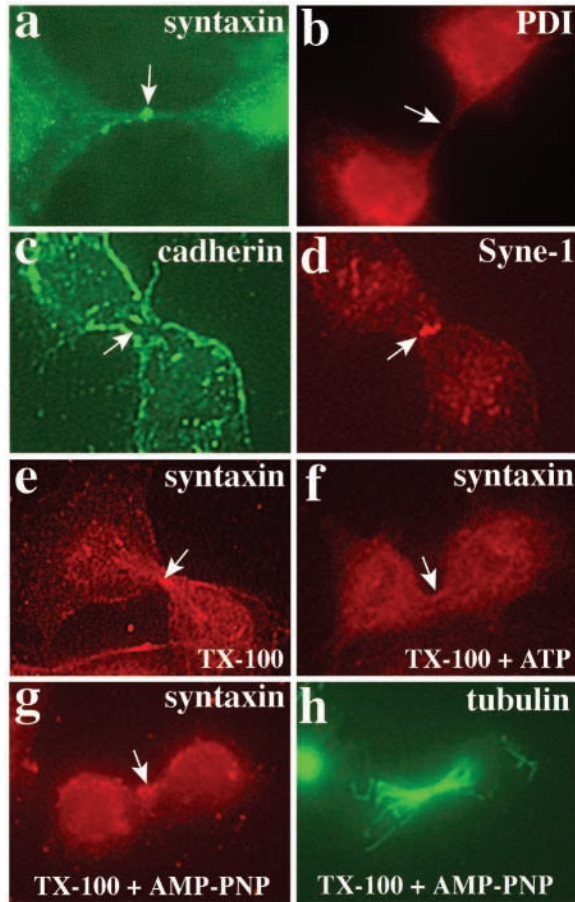
**Fig. 8.** Syntaxin localizes to the central spindle and midbody during anphase and cytokinesis. NRK cells in late stages of mitosis were fixed and stained with antibodies against syntaxin (a,e,f,g) protein disulfide isomerase (PDI) (b), E-cadherin (c). Cells stained for cadherin were also double stained with anti-Syne-1 to visualize the central spindle (arrow) (d). Syntaxin, concentrates in the midbody during cytokinesis (a,e,g), similar to Syne-1 and kinesin II. By contrast, accumulation within the midbody was not observed for PDI (arrow) (b) or E-caherin (arrow ) (c). (e-h) Cells extracted with TX-100 before fixation with (f) or without (e) ATP, or with non-hydrolyzable ATP analog AMP-PNP (g,h). Cells treated AMP-PNP were double stained with anti-syntaxin (g) and anti-tubulin (h) antibodies. Notice that, as we have observed with KIF3B and Syne-1, syntaxin association with the midbody is resistant to TX-100 extraction (e, arrow), greatly reduced in the presence of ATP (f, arrow), and stabilized in the presence of non-hydrolyzable ATP (g, arrow)

(Fig. 8a, arrow). Moreover, spindle-localized syntaxin was resistant to detergent-extraction (Fig. 8e) diminished in the presence of MgATP (Fig. 8f) and stabilized on extraction with AMP-PNP (Fig. 8g). These results support the conclusion that, like Syne-1, syntaxin associates with the mitotic spindle during cytokinesis through interactions with kinesin II.

As a more direct test of the potential role of KIF3B and Syne-1 in linking syntaxin-containing membranes to the spindle midbody, we examined the localization of syntaxin in cells transfected with recombinant KIF3B and Syne-1 fragments (Fig. 9). In mock-transfected cells and in cells transfected with full length KIF3B, syntaxin was enriched at the midbody (Fig.
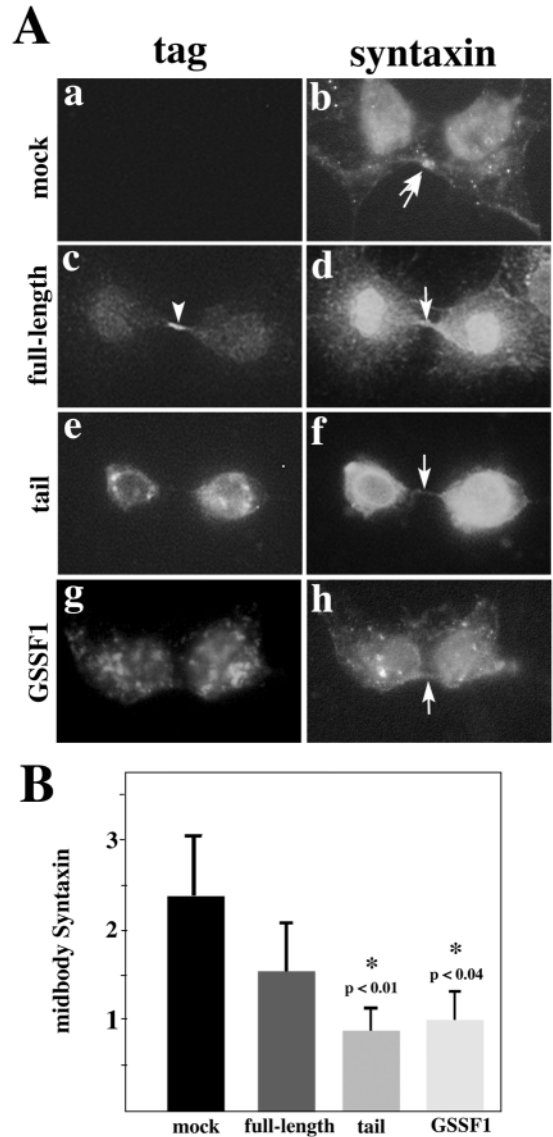


**Fig. 9.** Dominant-negative KIF3B and Syne-1 fragments block syntaxin localization to the midbody. (A) Enriched mitotic NRK cells were either mock-transfected (a,b) or transfected with myc-tagged full-length KIF3B (c,d), myc-tagged KIF3B tail domain (e,f), or HA-tagged Syne-1 fragment GSSF1 (g,h). Cells were fixed and stained with anti-myc (a,c,e) or anti-HA (g) antibodies to identify transfected cells, and with anti-syntaxin (b,d,f,h). As observed with Syne-1 localization under these conditions (Fig. 7), syntaxin was easily detected at the midbody in mock transfected cells (b, arrows) and in cells transfected with the control full-length KIF3B (d, arrow). However, in cells transfected with KIF3B tail (f, arrow) or GSSF1 (h, arrow), syntaxin was significantly reduced from the midbody region. (B) To quantify these results, examples of mock transfected cells, cells transfected with full-length KIF3B (full-length), KIF3B tail (tail) and GSSF1 were subjected to digital image analysis as described for Fig. 7e (* indicates statistically significant difference from mock transfected cells by Student's $t$-test).

9A, panels b,d). Notice that myc-tagged full-length KIF3B also localized to the midbody (Fig. 9A, panel c), indicating that the recombinant protein was functional. Quantitative analysis of these images (Fig. 9B) revealed no statistically significant

difference in the levels of midbody syntaxin in mock-transfected cells compared with cells expressing the full-length kinesin (P=0.13). By contrast, expression of the KIF3B tail domain resulted in a significant reduction of syntaxin at the midbody (Fig. 9A, f). Under these conditions the ratio of midbody syntaxin compared to the ratio of cytoplasmic syntaxin was ~1 (Fig. 9B), indicating that KIF3B tail expression reduced the level of midbody syntaxin to the maximal extent detectable with this assay. This result, together with the detergent- and ATP-dependence of syntaxin localization discussed above, provides compelling evidence that syntaxin-containing vesicles associate with the midbody through interactions with trimeric kinesin II. In addition, we also found that midbody syntaxin was reduced to an identical extent upon expression of the dominant-negative Syne-1 fragment GSSF1 (Fig. 9A, panel h, and Fig. 9B, GSSF1), providing evidence that Syne-1 also participated in the interaction of syntaxin with the midbody, perhaps by linking syntaxin-containing vesicles to KIF3B. Finally, notice that cleavage furrows were evident in cells expressing either GSSF1 or KIF3B tail (Fig. 9A, panels e-h), indicating that neither of these fragments affect cytokinesis by preventing cleavage furrow ingression.

## Discussion

We have found that expression of a kinesin-II-binding, dominant negative fragment of Syne-1 leads to an accumulation of binucleate cells. This result suggests a role for Syne-1 and kinesin II in cytokinesis because bi- and multinucleate cells have been identified following the disruption of cytokinesis in a range of organisms including yeast (Wang et al., 2002), *C. elegans* (Skop et al., 2001) and in mammalian cells (Fontijn et al., 2001; Matuliene and Kuriyama, 2002). Additional evidence for a role of Syne-1 and KIF3B in cytokinesis comes from our demonstration of their localization to the central spindle and the midbody during mitosis. Localization of Syne-1 and KIF3B to these structures is significant because perturbations in the structural integrity of the central spindle and midbody cause defects in cytokinesis (Adams et al., 1998; Giansanti et al., 1998; Matuliene and Kuriyama, 2002; Raich et al., 1998; Wheatley and Wang, 1996). Furthermore, several proteins that localize to these structures including RB6K (Hill et al., 2000), CHO1 (MKLP1, Matuliene and Kuriyama, 2002), ZEN-4 (Severson et al., 2000), Pav (Adams et al., 1998) and CYK-4 (Jantsch-Plunger et al., 2000) have been implicated in cytokinesis. Thus, the fact that Syne-1 and KIF3B localize to the central spindle and midbody, together with our expression studies with dominant negative fragments, provide compelling evidence of a role for Syne-1 and kinesin II in cytokinesis.

Our results indicate that Syne-1 and KIF3B function together during cytokinesis. The two dominant negative fragments used in this study, the Syne-1 fragment GSSF1 and the KIF3B tail domain, were found to associate with each other in a yeast two hybrid system and in co-pricipitation assays. Also, ectopically expressed GSSF1 was found to localize to punctate cytoplasmic structures (Fig. 2) that accumulate KIF3B, thus providing further evidence for an interaction between the two molecules. Furthermore, we found that both Syne-1 and KIF3B associate with the central spindle and midbody in a detergent resistant and ATP sensitive manner, and

overexpression of the KIF3B tail domain results in a dramatic reduction in the accumulation of Syne-1 at the midbody. Thus, we conclude that the mechanism of action of these proteins during cytokinesis will probably involve the direct coupling of Syne-1 and kinesisn II.

The structural integrity of both central spindle and midbody has been found to be crucial for cytokinesis (Giansanti et al., 1998; Matuliene and Kuriyama, 2002; Wheatley and Wang, 1996), suggesting that one potential function for kinesin II and Syne-1 is to physically stabilize these structures. However, an alternative role for Syne-1 in cytokinesis is suggested by the fact that all spectrin family members interact with membranes, raising the possibility that Syne-1 links membrane vesicles to the mitotic spindle during cytokinesis. It is well established that membrane vesicle movements and fusion are essential for cytokinesis in plant cells and there is growing evidence that vesicular trafficking is also important for cytokinesis animal cells (reviewed in Field et al., 1999; O'Halloran, 2000). Well known constituents of the membrane trafficking apparatus such as clathrin, dynamin, clathrin adaptors, syntaxin, arf and the exocyst complex are all implicated in cytokinesis (O'Halloran, 2000). Also, recent studies examining membrane vesicle motility in dividing *C. elegans* early embryos provided evidence that a specific recruitment of vesicles to the spindle region occurs after metaphase (Skop et al., 2001). This is precisely the same time frame that we observed the accumulation of Syne-1 at the central spindle. Our observation that midbody accumulation of vesicles containing syntaxin (a plasma membrane protein involved in vesicle fusion events) is detergent resistant, ATP sensitive and reduced upon expression of KIF3B tail domain or GSSF1 suggests that Syne-1-kinesin II facilitates vesicle transport along the spindle. In fact, a role for kinesin II in mediating vesicular transport along the mitotic spindle has been suggested previously by studies examining the distribution of the sea urchin homolog $KRP_{(85/95)}$ during cell division (Henson et al., 1995). We speculate that Syne-1 can serve to link membrane vesicles to kinesin II, which can then facilitate the transport of these vesicles and associated Syne-1 along spindle-microtubules to the central spindle and midbody. Accumulated vesicles can then fuse with each other and with the cleavage furrow membrane to facilitate the fission of daughter cells.

The close association of Syne-1 and the actin-based contractile ring during cytokinesis suggests an alternative or additional role for these proteins. Our results indicate that Syne-1 associates with the midbody to form a discrete ring that is concentric with and in close opposition to the contractile ring. This localization raises the possibility that Syne-1 might serve to tether the contractile ring to the midbody, a feasible role for an elongated protein like Syne-1 with widely separated KIF3B and actin binding sites. Such an activity could serve to facilitate cytokinesis by stabilizing the contractile ring, keeping it in a contracted state tightly associated with the spindle midbody. Notice that the two roles we have proposed for Syne-1 in cytokinesis, vesicular trafficking and linking of contractile ring and midbody, are not mutually exclusive. It is indeed possible that Syne-1 can perform both functions simultaneously. In fact, it is not difficult to imagine how the endpoint of cytokinesis, cell fission, is greatly facilitated by a molecule that can both stabilize the interaction of the cleavage furrow with the spindle and recruit vesicle to the site for subsequent membrane fusion events.

Syne-1-kinesisn II interactions could also be significant in other functions proposed for Syne-1. While nuclear positioning events could be facilitated by Syne-1 through its capacity to bind the actin cytoskeleton (Starr and Han, 2002), there is also evidence that microtubule interactions are important in this function (Morris, 2003). Kinesin-dependent microtubule interactions of nuclear envelope-associated Syne-1 could provide the forces required to initiate nuclear motility. Also, we have found previously that the expression of dominant negative Syne-1 fragments leads to altered Golgi morphology (Gough et al., 2003). Because it is well known that Golgi morphology and cytoplasmic positioning is coupled to microtubules, this function of Syne-1 might also be facilitated by interactions with kinesin II. Finally, we have recently found evidence that Syne-1 is required for retrograde trafficking of Golgi-derived vesicles to the ER (Gough and Beck, submitted). KIF3B is involved in vesicle transport (Yamazaki et al., 1995) and kinesins are implicated in retrograde Golgi trafficking (Lippincott-Schwartz et al., 1995), an event that should involve plus-end directed microtubule motors.

## References

**Adams, R. R., Tavares, A. A., Salzberg, A., Bellen, H. J. and Glover, D. M.** (1998). Pavarotti encodes a kinesin-like protein required to organize the central spindle and contractile ring for cytokinesis. *Genes Dev.* **12**, 1483-1494.

**Apel, E. D., Lewis, R. M., Grady, R. M. and Sanes, J. R.** (2000). Syne-1, a dystrophin- and Klarsicht-related protein associated with synaptic nuclei at the neuromuscular junction. *J. Biol. Chem.* **275**, 31986-31995.

**Cooke, C. A., Heck, M. M. and Earnshaw, W. C.** (1987). The inner centromere protein (INCENP) antigens: movement from inner centromere to midbody during mitosis. *J. Cell Biol.* **105**, 2053-2067.

**Danilchik, M. V., Funk, W. C., Brown, E. E. and Larkin, K.** (1998). Requirement for microtubules in new membrane formation during cytokinesis of Xenopus embryos. *Dev. Biol.* **194**, 47-60.

**Field, C., Li, R. and Oegema, K.** (1999). Cytokinesis in eukaryotes: a mechanistic comparison. *Curr. Opin. Cell Biol.* **11**, 68-80.

**Fontijn, R. D., Goud, B., Echard, A., Jollivet, F., van Marle, J., Pannekoek, H. and Horrevoets, A. J.** (2001). The human kinesin-like protein RB6K is under tight cell cycle control and is essential for cytokinesis. *Mol. Cell. Biol.* **21**, 2944-2955.

**Giansanti, M. G., Bonaccorsi, S., Williams, B., Williams, E. V., Santolamazza, C., Goldberg, M. L. and Gatti, M.** (1998). Cooperative interactions between the central spindle and the contractile ring during *Drosophila* cytokinesis. *Genes Dev.* **12**, 396-410.

**Gough, L. L., Fan, J., Chu, S., Winnick, S. and Beck, K. A.** (2003). Golgi Localization of Syne-1. *Mol. Biol. Cell* **14**, 2410-2424.

**Henson, J. H., Cole, D. G., Terasaki, M., Rashid, D. and Scholey, J. M.** (1995). Immunolocalization of the heterotrimeric kinesin-related protein KRP(85/95) in the mitotic apparatus of sea urchin embryos. *Dev. Biol.* **171**, 182-194.

**Hill, E., Clarke, M. and Barr, F. A.** (2000). The Rab6-binding kinesin, Rab6-KIFL, is required for cytokinesis. *EMBO J.* **19**, 5711-5719.

**Hirose, K., Kawashima, T., Iwamoto, I., Nosaka, T. and Kitamura, T.** (2001). MgcRacGAP is involved in cytokinesis through associating with mitotic spindle and midbody. *J. Biol. Chem.* **276**, 5821-5828.

**Jantsch-Plunger, V. and Glotzer, M.** (1999). Depletion of syntaxins in the early *Caenorhabditis elegans* embryo reveals a role for membrane fusion events in cytokinesis. *Curr. Biol.* **9**, 738-745.

**Jantsch-Plunger, V., Gonczy, P., Romano, A., Schnabel, H., Hamill, D., Schnabel, R., Hyman, A. A. and Glotzer, M.** (2000). CYK-4: A Rho family GTPase activating protein (GAP) required for central spindle formation and cytokinesis. *J. Cell Biol.* **149**, 1391-1404.

**Kreis, T. E.** (1990). Role of microtubules in the organisation of the Golgi apparatus. *Cell. Motil. Cytoskeleton* **15**, 67-70.

**Lippincott-Schwartz, J., Cole, N. B., Marotta, A., Conrad, P. A. and Bloom, G. S.** (1995). Kinesin is the motor for microtubule-mediated Golgi-to-ER membrane traffic. *J. Cell Biol.* **128**, 293-306.

**Matuliene, J. and Kuriyama, R.** (2002). Kinesin-like protein CHO1 is required for the formation of midbody matrix and the completion of cytokinesis in mammalian cells. *Mol. Biol. Cell.* **13**, 1832-1845.

**Mislow, J. M., Kim, M. S., Davis, D. B. and McNally, E. M.** (2002). Myne-1, a spectrin repeat transmembrane protein of the myocyte inner nuclear membrane, interacts with lamin A/C. *J. Cell Sci.* **115**, 61-70.

**Mitchison, T. J.** (1988). Microtubule dynamics and kinetochore function in mitosis. *Annu. Rev. Cell. Biol.* **4**, 527-549.

**Morris, N. R.** (2003). Nuclear positioning: the means is at the ends. *Curr. Opin. Cell Biol.* **15**, 54-59.

**Nasmyth, K.** (2002). Segregating sister genomes: the molecular biology of chromosome separation. *Science* **297**, 559-565.

**O'Halloran, T. J.** (2000). Membrane traffic and cytokinesis. *Traffic* **1**, 921-926.

**Raich, W. B., Moran, A. N., Rothman, J. H. and Hardin, J.** (1998). Cytokinesis and midzone microtubule organization in *Caenorhabditis elegans* require the kinesin-like protein ZEN-4. *Mol. Biol. Cell* **9**, 2037-2049.

**Rappaport, R.** (1986). Establishment of the mechanism of cytokinesis in animal cells. *Int. Rev. Cytol.* **105**, 245-281.

**Severson, A. F. and Bowerman, B.** (2002). Cytokinesis: closing in on the central spindle. *Dev. Cell* **2**, 4-6.

**Severson, A. F., Hamill, D. R., Carter, J. C., Schumacher, J. and Bowerman, B.** (2000). The aurora-related kinase AIR-2 recruits ZEN-4/CeMKLP1 to the mitotic spindle at metaphase and is required for cytokinesis. *Curr. Biol.* **10**, 1162-1171.

**Shima, D. T., Cabrera-Poch, N., Pepperkok, R. and Warren, G.** (1998). An ordered inheritance strategy for the Golgi apparatus: visualization of mitotic disassembly reveals a role for the mitotic spindle. *J. Cell Biol.* **141**, 955-966.

**Skop, A. R., Bergmann, D., Mohler, W. A. and White, J. G.** (2001). Completion of cytokinesis in *C. elegans* requires a brefeldin A-sensitive membrane accumulation at the cleavage furrow apex. *Curr. Biol.* **11**, 735-746.

**Starr, D. A. and Han, M.** (2002). Role of ANC-1 in tethering nuclei to the actin cytoskeleton. *Science* **298**, 406-409.

**Thyberg, J. and Moskalewski, S.** (1998). Partitioning of cytoplasmic organelles during mitosis with special reference to the Golgi complex. *Microsc. Res. Tech.* **40**, 354-368.

**Wang, H., Tang, X., Liu, J., Trautmann, S., Balasundaram, D., McCollum, D. and Balasubramanian, M. K.** (2002). The multiprotein exocyst complex is essential for cell separation in *Schizosaccharomyces pombe*. *Mol. Biol. Cell* **13**, 515-529.

**Wheatley, S. P. and Wang, Y.** (1996). Midzone microtubule bundles are continuously required for cytokinesis in cultured epithelial cells. *J. Cell Biol.* **135**, 981-989.

**Yamazaki, H., Nakata, T., Okada, Y. and Hirokawa, N.** (1995). KIF3A/B: a heterodimeric kinesin superfamily protein that works as a microtubule plus end-directed motor for membrane organelle transport. *J. Cell Biol.* **130**, 1387-1399.

**Zhang, Q., Ragnauth, C., Greener, M. J., Shanahan, C. M. and Roberts, R. G.** (2002). The nesprins are giant actin-binding proteins, orthologous to *Drosophila melanogaster* muscle protein MSP-300. *Genomics* **80**, 473-481.

**Zhang, Q., Skepper, J. N., Yang, F., Davies, J. D., Hegyi, L., Roberts, R. G., Weissberg, P. L., Ellis, J. A. and Shanahan, C. M.** (2001). Nesprins: a novel family of spectrin-repeat-containing proteins that localize to the nuclear membrane in multiple tissues. *J. Cell Sci.* **114**, 4485-4498.